Available online at www.sciencedirect.com

ScienceDirect

Physics Procedia 74 (2015) 254 – 260

Physics Procedia

Conference of Fundamental Research and Particle Physics, 18-20 February 2015, Moscow, Russian Federation

The prototype of detector for registration neutron fluxes initiated by electrons and protons of high energy in the calorimeter

I.I. Gnezdilov*, V.V. Kadilin, A.A. Kaplun, A.A. Taraskin

National Research Nuclear University MEPhI (Moscow Engineering Physics Institute),Kashirskoe Shosse 31, Moscow 115409, Russia

Abstract

A prototype of detector for neutron fluxes, induced by electron and proton showers, registration has been designed. Neutron detector (ND) consists of three alternating layers composed of cadmium plates and plastic scintillator. An optimal detector solution based on a mathematical simulation has been proposed. This article contains technical information and a description of the experiment to determine neutron detection efficiency, as well as experimental and simulation data analysis results.

Peer-review under responsibility of the National Research Nuclear University MEPhI (Moscow Engineering Physics Institute)

Keywords: calorimeter; Cd; electron; gamma-ray; hadron; neutron detector; plastic scintillator; rejection; shower

1. Introduction

Calorimeters are widely used in particle physics. It is an instrument to determine particles type and energy, as well as to perform spatial measurements. Structurally these are blocks of medium, where particles lose energy during their movement, because of different kinds of interactions. As a result, primary particles produce cascades of secondary particles. Thus, a calorimeter should provide significant moderation of certain types of particles retaining the ability to measure these energy losses.

Electrons, positrons and gamma-rays produce electromagnetic showers during the moderation process. A photon may produce an electron-positron pair. In turn, if an energy of these electrons (positrons) is larger than a certain threshold, they will produce bremsstrahlung (photons), thereby a number of particles in a shower will increase until their average energy falls below a critical one, and then the ionization will become the main mechanism. Neutrons

* Corresponding author. Tel.: +7-495-788-56-99.
E-mail address: y.gnezdilov@gmail.com

Peer-review under responsibility of the National Research Nuclear University MEPhI (Moscow Engineering Physics Institute)
doi:10.1016/j.phpro.2015.09.224

are being produced during a shower progression due to photonuclear reactions.

Showers produced by hadrons have more complex structure than electron-produced ones. When a high-energy hadron enters a nucleus, it interacts with its nucleons and transfers part of its energy to them. A great quantity of neutrons is produced in interactions of high-energy hadrons and nuclei with medium nuclei (especially with heavy nuclei), along with charged particles. Considering the kinematics of such interactions, one can select three basic regions of particles production as a first approximation. The first region is related to fragmentation of an incident nucleus, when neutrons are produced in a narrow forward cone along the beam with energies close to the energy of a projectile particle, which is reduced by one nucleon. Here, the elastic and quasi-elastic interaction with charge-exchange of incident protons can be attributed. The second region, which forms hard neutron spectrum at large angles, is a region of intersection of colliding nuclei, which is a zone of interaction of nucleon participants of collision. Target residual nucleus decay results in a low-energy neutron emission, which is close to an isotropic one, and represents the third region of neutron production [1]. Hadron cascades produce significantly more neutrons than electromagnetic ones. Thus, in order to separate proton and electron showers in a calorimeter, one can use a neutron count. A neutron detector (ND) should be placed under a calorimeter given that a primary particle (electron or proton) falls vertically on a calorimeter entering surface.

In order to precisely characterize the neutron component associated with the different types of showers, a detailed Monte Carlo simulation has been performed using the FLUKA simulation package. The CALET BGO homogeneous calorimeter, consisting of a BGO tower ($60\times60\times30$ cm^3) with a vertical depth of approximately 30cm has been simulated as a "test detector"(Fig. 1). For each simulated event the produced neutrons have been propagated till they reached the outside of the calorimeter. The energy, direction and arrival time of each neutron exiting the calorimeter from the bottom side, where the moderator is placed, were logged for further use. In Fig. 2 the number of neutrons exiting from the calorimeter is shown for 1 TeV interacting protons and for 400 GeV electrons (1 TeV proton showers give the same calorimetric signal as 400 GeV electrons in BGO on average). The rejection factor achievable for hadronic showers can be as high as ~ 10^3 considering the neutron counting. The bulk of neutrons originate from the excitation and de-excitation of nuclei and exhibit a maximum in the MeV energy region (Fig. 3). Many neutrons undergo moderation before escaping and their energy is consequently degraded down to the eV energy region. Some neutrons can also be produced promptly in the hadronic interactions along the shower core, with an energy reaching that of the primary proton. The highest energy neutrons (E > 10 MeV) arrive simultaneously with the charged component of the shower, while the low energy and more abundant component arrives into the neutron detector with a delay ranging from 10 to 1000 ns and, thus, can be easily identified. The figure for electromagnetic showers is similar but with a much reduced contribution for the prompt neutron emission [2].

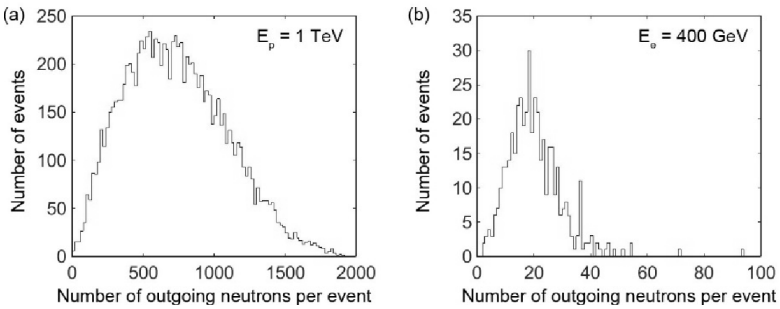

Fig. 1. Neutron yield outside the CALET calorimeter for (a) 1 TeV interacting protons and (b) 400 GeV electrons [2].

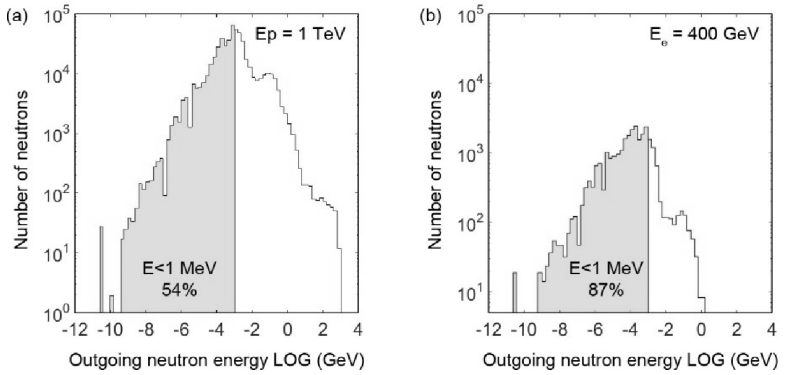

Fig. 2. Energy spectrum of outgoing neutrons outside the CALET calorimeter for (a) 1 TeV interacting protons and (b) 400 GeV electrons [2].

2. The design of the prototype ND

Simulation models of the ND (Fig. 3) are composed of alternating layers of polystyrene plastic scintillator (PS) [3] and 200 μm thick cadmium layers. The entering surface of the ND has dimensions of 80×80 cm^2 and thickness of 5 cm. PS was used as a neutron moderator medium.

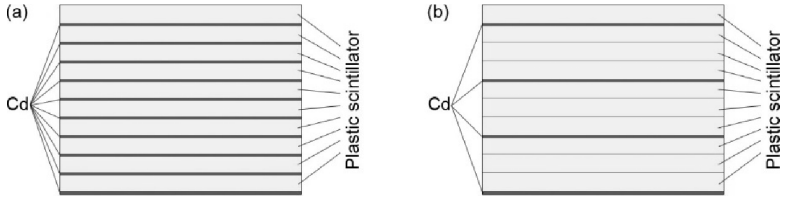

Fig. 3. Prototype ND design. Cd sheets are arranged in (a) one layer PS and (b) three layers PS.

Neutrons are detected by PS layers because of the (n, γ) reaction of a cadmium nuclei. 4.1 gamma-particles are produced in each act of capture on average. Such particles have energies ranging from 0.01 up to 9 MeV. Fig. 4 demonstrates the energy dependence of the (n, γ) reaction cross section. As seen, the reaction cross section is significant not only for low energy (< 0.4 eV) neutrons, where it reaches 2500 barn, but also for the entire incident neutron flux. Thus the (n, γ) reaction photons can be observed from both moderated and fast neutrons. Fig. 5 shows the energy distribution of (n, γ) photons.

Fig. 6 shows that the scintillator light is gathered using spectrum WLS fibers (Kuraray Y-11) with 1 mm section. Fibers are glued into grooves on the PS surface with 10 mm step and 2 mm depth [4]. Light detection is performed by SiPMs [5].

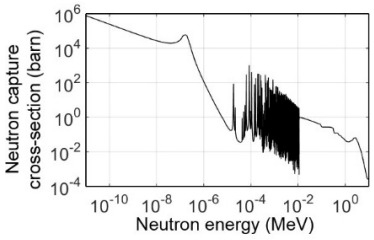

Fig. 4. Cd (n, γ) reaction cross-section as a function of neutron energy.

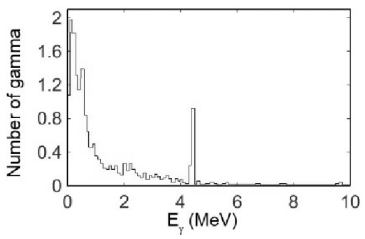

Fig. 5. Cd (n, γ) reaction photons energy distribution.

Fig. 6. Scintillator light gathering in the PS layer using WLS fibers.

3. GEANT4 simulation and results

The optimal ND construction was chosen with instrumentality of mathematical modeling using GEANT4. It was assumed that a neutron is detected when the energy loss of the electron, produced by the (n, γ) reaction photon, is larger than a certain threshold. Thus, the total energy loss of produced electrons was calculated. A plane-parallel 1 MeV neutron flux was oriented perpendicular to the detector largest surface. Total statistics of neutrons ranged from 10^2 to 10^6. Gamma-particles counted as detected regardless of which cadmium layer produced a photon. The electron energy loss threshold to discriminate the gamma-ray background was set to 2.5 MeV.

Neutron detection efficiency dependence on the thickness of the cadmium layers was calculated to determine the optimal thickness value (Fig. 3(a)). Fig. 7 shows that when the thickness increases from 0.1 mm to 0.5 mm, the efficiency increases by 10% only. Thus, it one can conclude that the cadmium layer thickness in such range has only little impact on the detection efficiency.

The gamma-ray detection efficiency is low, because nuclei composing PS medium have low atomic number. By increasing the overall thickness and, as a consequence, the mass of the ND, we may achieve better neutron detection efficiency with the current ND design. Calculations were made for the different values of the ND thickness. Fig. 8 demonstrates the obtained results. Thus, the increase of the PS thickness up to 15 cm also increases the neutron detection efficiency to 20%. Another way to increase the detection efficiency is to lower the energy threshold for secondary electrons to 1 MeV and lower. Fig. 9 shows the efficiency on a threshold level in the range of 1 to 2.5 MeV. As one can notice, the efficiency increases by a factor of four when the threshold decreases by a factor of 2.5.

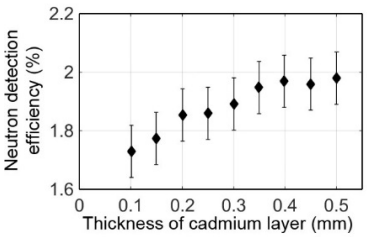

Fig. 7. Detection efficiency as a function of thickness of cadmium layer.

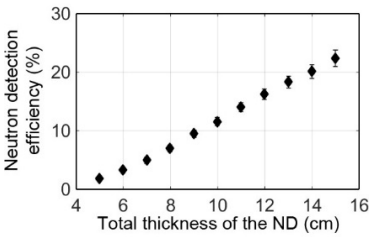

Fig. 8. Detection efficiency as a function of thickness of the ND.

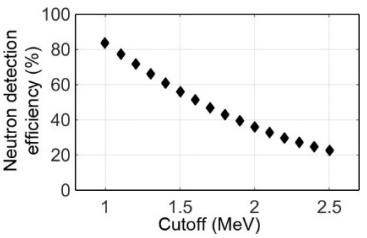

Fig. 9. Detection efficiency as a function of the secondary electrons energy release cutoff.

Detection efficiency for different cadmium arrangements was also calculated. Three different arrangements, where each one of cadmium layers alternating with one, two or three PS layers for 40x40 cm^2 and 80x80 cm^2 models were simulated. Overall thickness of the layers in each model was equal to 15 cm.

Plots of the detection efficiency of the cadmium layers after 1 and 3 layers of PS model dimensions 80×80cm^2 are shown in Fig. 10(a) and, for the dimensions of 40×40 $cm^2$are shown in Fig. 10(b).

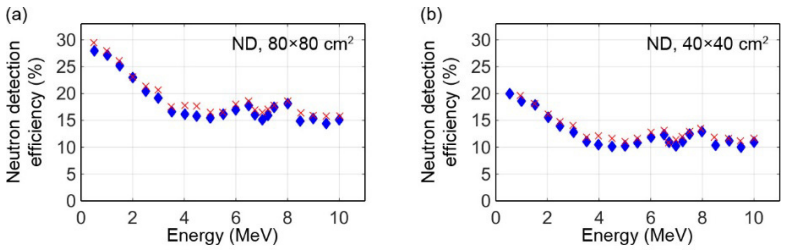

Fig. 10. Detection efficiency as a function of energy neutrons (× — after 1 layer PS, ♦ — after 3 layers PS): (a) for model dimensions 80×80 cm^2 and (b) for model dimensions 40×40 cm^2.

As can be seen, the detection efficiency for different number of cadmium layers is almost identical for each model. Decreasing of model size twice (from 80×80 cm^2 to 40×40 cm^2) decreases the overall efficiency by 10%.

4. Experiment and discussion

To confirm the simulation results and to study the ND parameters, an experiment scheme was developed, shown in Fig. 11. A pulsed neutron generator ING-101 with 0.8 μs pulse width and the neutron flux of 5×10^6 1/s was used in the experiment. Energy of neutrons equals to 2.2 MeV for a deuterium target. A pulse generator G5-88 was used to run the ING and to control the repetition rate of neutron pulses (1 to 30 Hz). A signal was given by ING to the first oscilloscope input to compare the generation time of the pulse with the neutron detection event. The neutron pulse appearance was controlled by a radiation monitor containing neutron moderator and a LiI(Eu) neutron detector. The latter was calibrated so that a single neutron detector pulse corresponded to fluence equal to one neutron per cm^2. The neutron detector was placed on one axial line with the ING at a distance of 1.33 m. Separation of gamma-rays, produced during a pulse from a capture gamma-rays, was performed through 5 μs event registration delay. Fig. 12 shows number of events in the time gap of 2 μs. Measurements were conducted with and without the use of additional polyethylene moderator. Comparison of the results leads to the conclusion that the use of additional moderator has virtually no effect on the neutron detection efficiency.

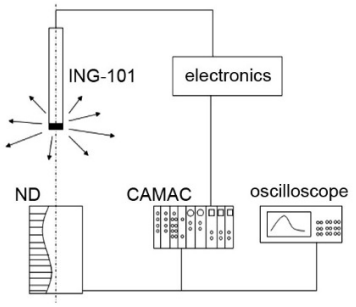

Fig. 11. The scheme of the experiment.

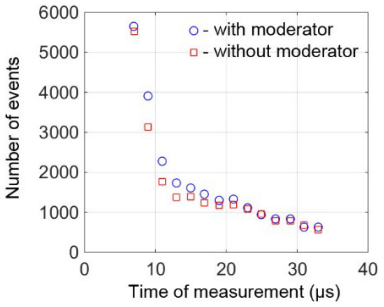

Fig. 12. Number of events as a function of measurement time.

The detection efficiency of the 24×20×4.5 cm^3 ND was calculated. This detector has been used for laboratory tests of the physical model, which consists of 7 layers of cadmium and 8 polystyrene layers. The ND got a plane-parallel neutron flux of 2.2 MeV neutrons. Table 1 shows the efficiency values for different cadmium layers positions (alternating with 1, 2, 3 or 4 layers of PS).

Table 1. Neutron detection efficiency for ND with different cadmium layers.

ND	Neutron detection efficiency, %
ND: Cd layers are arranged in one layer PS	1.9
ND: Cd layers are arranged in two layers PS	1.7
ND: Cd layers are arranged in three layers PS	1.6
ND: Cd layers are arranged in four layers PS	1.2

The table 1 demonstrates that the detection efficiency drops with the number of cadmium layers decrease, but it seems feasible to place cadmium plates alternating with two layers of scintillator to reduce the weight of ND. The detection efficiency of this model ranges from 1% to 2% with a relative error of ±0.1%. The low efficiency could be due to a substantial width of the gamma-rays energy spectrum produced during the (n, γ) reaction. Such particles have an energy range from 0.01 to 9 MeV (Fig. 5), although for a neutron detection only rays with energy greater than 2.5 MeV can be used.

Neutron detection efficiency of the experimental and the calculation model of the ND as a function of the event collection time is shown in Fig. 13.

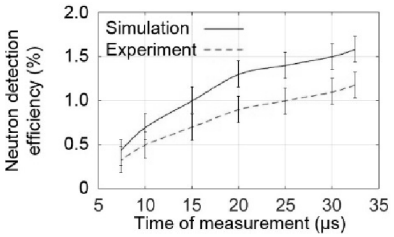

Fig. 13. Neutron detection efficiency function for the ND containing 7 cadmium layers and 8 layers of PS.The delay (reference) time is 5 μs (no additional moderator).

Experimental detection efficiency of the prototype is ~1.2±0.3% during the 32 μs event collection interval. Based on the data obtained one can see that the calculated efficiency value (1.7 ± 0.3%) is slightly larger than the experimental result. The dependence trend coincides with the measured one. The pulse duration and the distribution of neutrons in it were not taken into account in the calculations. The number of neutrons in the pulse was determined by the monitor reading, so there may be a non-excluded systematic error.

5. Conclusions

Taking into account that high-energy particle detectors and, in particular, calorimeters are widely used in space experiments and cosmic radiation measurements, it may be prudent to use compact and fast neutron detectors as a part of some larger space instruments. The PAMELA experiment proved that even a relatively slow helium neutron detector could be a very effective tool for hadron/electron discrimination (i.e. high-energy particles identification) [6]. This is a significant process considering that a number of background solar protons is by far greater than a number of “useful” events. Thereby such multi-layered detector construction may find its place in the GAMMA-400 gamma-ray telescope for electron/hadron rejection [7], which is scheduled for launch in the early 2020s.

Acknowledgements

The authors thank their colleagues Vasiliy Mukhin and Grigoriy Dedenko for help in the preparation of this article and for help with simulation.

References

[1] Yurevich V.I. Production of Neutrons in Thick Targets by High-Energy Protons and Nuclei. *Physics of Particles and Nuclei* 2010;41(5): 778–825.
[2] Bottai S., Castellini G., Papini P. *et al.* An innovative approach to compact calorimetry in space, NEUCAL. *Nuclear Instruments and Methods in Physics Research A* 2010;617:464–466.
[3] Britvich G.I., Brehovskih V.V., Semenov V.K. *et al.* Basic properties of polystyrene scintillators produced in IHEP and detectors based on them. Instruments and Experimental Techniques 2015;2:47-57.
[4] Ampilogov N.B. Amelchakov M.B., Britvich G.I. *et al.* Scintillation detector with obtaining information from the optical fiber. 30th RCRC, St. Petersburg 2008;1–8.
[5] SensL C-Series Low Noise, Fast, Blue-Sensitive Silicon Photomultipliers Datasheet, *http://www.sensl.com/downloads/ds/DS-MicroCseries.pdf* 2014;17.
[6] Boezio M., Pearce M., Albi M. *et al.* The electron–hadron separation performance of the PAMELA electromagnetic calorimeter. Astroparticle Physics 2006;26:111–118.
[7] Leonov A.A., Galper A.M., Bonvicini V. *et al.* A separation of electrons and protons in the GAMMA-400 gamma-ray telescope. arXiv:1503.06657v1 [astro-ph.IM] 2015.